

A new algorithm to determine the creation or depletion term of parabolic equations from boundary measurements^{*}

Loc Hoang Nguyen

Department of Mathematics and Statistics, University of North Carolina at Charlotte, Charlotte, NC, 28223, USA,

ARTICLE INFO

Keywords:
coefficient inverse problem
parabolic equations
approximation
Fourier coefficients

Abstract

We propose a robust numerical method to find the coefficient of the creation or depletion term of parabolic equations from the measurement of the lateral Cauchy information of their solutions. Most papers in the field study this nonlinear and severely ill-posed problem using optimal control. The main drawback of this widely used approach is the need of some advanced knowledge of the true solution. In this paper, we propose a new method that opens a door to solve nonlinear inverse problems for parabolic equations without any initial guess of the true coefficient. This claim is confirmed numerically. The key point of the method is to derive a system of nonlinear elliptic equations for the Fourier coefficients of the solution to the governing equation with respect to a special basis of L^2 . We then solve this system by a predictor-corrector process, in which our computation to obtain the first and second predictors is effective. The desired solution to the inverse problem under consideration follows.

1. Introduction

Let Ω be a cube $(-R, R)^d \subset \mathbb{R}^d$, $d \geq 2$, where R is a positive number. Introduce a $d \times d$ matrix valued function A with entries in the class $C^1(\mathbb{R}^d, \mathbb{R}^{d \times d})$. Assume throughout the paper that

1. A is symmetric; i.e, $A^T = A$,
2. the matrix A is uniformly elliptic; i.e., there exists a positive number μ such that

$$A(\mathbf{x})\xi \cdot \xi \geq \mu|\xi|^2 \quad \text{for all } \mathbf{x}, \xi \in \mathbb{R}^d,$$

3. for all $\mathbf{x} \in \mathbb{R}^d \setminus \Omega$, $A(\mathbf{x}) = \text{Id}$ where Id is the identity matrix.

Let \mathbf{b} be a d -dimensional vector valued function in $C^1(\mathbb{R}^d, \mathbb{R}^d) \cap L^\infty(\mathbb{R}^d, \mathbb{R}^{d \times d})$. Define the operator

$$Lw(\mathbf{x}) = \text{div}(A(\mathbf{x})\nabla w(\mathbf{x})) + \mathbf{b} \cdot \nabla w(\mathbf{x}) \quad \text{for all } w \in H^2(\mathbb{R}^d), \mathbf{x} \in \mathbb{R}^d.$$

Consider the solution u to the following initial value problem for the following parabolic equation

$$\begin{cases} u_t(\mathbf{x}, t) = Lu(\mathbf{x}, t) + c(\mathbf{x})u(\mathbf{x}, t) & \mathbf{x} \in \mathbb{R}^d, t \in [0, \infty], \\ u(\mathbf{x}, 0) = f(\mathbf{x}) & \mathbf{x} \in \mathbb{R}^d. \end{cases} \quad (1)$$


The second order term $\text{div}(A(\mathbf{x})\nabla u(\mathbf{x}, t))$ describes the diffusion, the first order term $\mathbf{b}(\mathbf{x}) \cdot \nabla u(\mathbf{x}, t)$ describes the transport and the zeroth order term $c(\mathbf{x})u(\mathbf{x}, t)$ describes creation or depletion. In this paper, we numerically solve the problem of reconstructing the coefficient $c(\mathbf{x})$ of the creation or depletion term. More precisely, we propose a method to solve the highly nonlinear and severely ill-posed coefficient inverse problem.

Problem 1.1 (Coefficient Inverse Problem (CIP)). *Assume that $f(\mathbf{x}) \neq 0$ for all $\mathbf{x} \in \Omega$. Given a time $T > 0$ and the lateral Cauchy data*

$$F(\mathbf{x}, t) = u(\mathbf{x}, t) \quad \text{and} \quad G(\mathbf{x}, t) = \partial_\nu u(\mathbf{x}, t) \quad (2)$$

for all $\mathbf{x} \in \partial\Omega$ and $t \in [0, T]$, determine the coefficient $c(\mathbf{x})$, $\mathbf{x} \in \Omega$. Here ν is the outward normal vector of $\partial\Omega$.

^{*}This work is supported by US Army Research Laboratory and US Army Research Office grant W911NF-19-1-0044.

 loc.nguyen@uncc.edu (L.H. Nguyen)

ORCID(s):

Problem 1.1 has uncountable applications in the reality. In fact, suppose that interior points of a medium are not accessible. In this case, by measuring both the function u and the flux at the boundary of that medium for a certain period of time and by solving Problem 1.1, one can determine the coefficient $c(\mathbf{x})$ of the governing equation in (1), which enables us to inspect that medium without destructing it. We recall here a specific example in bioheat transfer. In this field, the coefficient $c(\mathbf{x})$ represents the blood perfusion. The knowledge of this coefficient plays a crucial role in calculating the temperature of the blood flowing through the tissue, see [1]. The uniqueness of Problem 1.1 is still open and considered as an assumption of in this paper. One can find the uniqueness of other versions of Problem 1.1 in [2, 3, 4] when some internal data are assumed to be known. When the Dirichlet to Neuman map is given, the reader can find the uniqueness in [5]. Another related problem is the inverse problem of recovery from the measurement of the final time for parabolic equations. This problem is very important and interesting, see [6, 7, 8, 9, 10] for theoretical results and numerical methods.

Coefficient inverse problems for parabolic equations were studied intensively. Up to the knowledge of the author, the widely used method to solve this problem is the optimal control approach, see e.g., [11, 12, 1, 13, 14] and references therein. The authors of [11] applied the optimal control method involving a preconditioner to numerically compute the heat conductivity with high quality. The main drawback of this method is the need of a good initial guess for the true solution while a good initial guess is not always available. On the other hand, we specially draw the reader's attention to the convexification method, see [15, 16], which can overcome the difficulty about the availability of the initial guess. In those papers [15, 16], the authors introduce a convex functional whose minimizer yields the solution of the problem under consideration, by combining the quasi-reversibility method and the Carleman weight functions. Great 1D numerical examples, illustrating the role of Carleman weight functions in convexifying the cost functionals, are presented in [15]. It is valuable to numerically test this convexification method in higher dimensions. We also cite to [17] for another method to solve Problem 1.1 by repeatedly solving its linearization. In the current paper, we propose a novel method in which no advanced knowledge about the true coefficient is required. This claim is numerically confirmed even in the case when the contrast is high. We therefore called the proposed method "global".

Our method to solve Problem 1.1 consists of two stages. In the first stage, we eliminate the function $c(\mathbf{x})$ from (1). The resulting equation obtained in this stage is not a standard equation. A numerical method to solve it is not available yet. We approximate it a coupled system of elliptic partial differential equations. This system is derived based on a truncation of the Fourier series, with respect to a special basis originally introduced in [18]. We apply a predictor-corrector procedure, in which the first approximation of the true solution is computed without any of its advance knowledge, to solve this system. The solution of Problem 1.1 follows.

Two important steps in our method require us to find vector valued functions satisfying a system of elliptic partial differential equations and both Dirichlet and Neumann boundary conditions. We employ the quasi-reversibility method for this purpose and we also prove the convergence of the quasi-reversibility method in our context, using a new Carleman estimate in [19]. The quasi-reversibility method was first introduced by Lattès and Lions in [20] for numerical solutions of ill-posed problems for partial differential equations. It has been studied intensively since then, see e.g., [21, 22, 23, 24, 25, 26, 27, 28, 29, 30, 19]. A survey on this method can be found in [31].

In Section 2, we derive the system mentioned above. In Section 3, we propose a numerical method to solve that system. Also in Section 3, we study the quasi-reversibility method that can be applied in our context. In Section 4, we describe the implementation using the finite difference method. In Section 5, we present some numerical results. Section 6 is for the concluding remarks.

2. A nonlinear coupled system of elliptic equations

From now on, we denote by Ω_T the set $\Omega \times [0, T]$. Define the function

$$v(\mathbf{x}, t) = u_t(\mathbf{x}, t) \quad \text{for all } (\mathbf{x}, t) \in \Omega_T. \quad (3)$$

It follows from (1) that

$$v_t(\mathbf{x}, t) = Lv(\mathbf{x}, t) + c(\mathbf{x})v(\mathbf{x}, t) \quad \text{for all } (\mathbf{x}, t) \in \Omega_T. \quad (4)$$

On the other hand, for all $\mathbf{x} \in \Omega$,

$$v(\mathbf{x}, 0) = u_t(\mathbf{x}, 0) = Lf(\mathbf{x}) + c(\mathbf{x})f(\mathbf{x}).$$

Therefore,

$$c(\mathbf{x}) = \frac{v(\mathbf{x}, 0) - Lf(\mathbf{x})}{f(\mathbf{x})} \quad \text{for all } \mathbf{x} \in \Omega. \quad (5)$$

Plugging (5) into (4), we obtain the following equation

$$v_t(\mathbf{x}, t) = Lv(\mathbf{x}, t) - \frac{Lf(\mathbf{x})}{f(\mathbf{x})}v(\mathbf{x}, t) + \frac{v(\mathbf{x}, 0)}{f(\mathbf{x})}v(\mathbf{x}, t) \quad (6)$$

for all $(\mathbf{x}, t) \in \Omega_T$.

Remark 2.1. Solving the nonlinear equation (6) is challenging due to the presence of the initial condition $v(\mathbf{x}, 0)$. A theoretical result to solve it is not yet available. We employ the technique of truncating the Fourier series, see [18], to solve (6).

Recall a special orthonormal basis of $L^2(0, T)$ originally introduced by Klivanov [18] in 2017. This basis plays a crucial role in deriving an approximate model whose solution will be used to directly compute the solution of Problem 1.1. For each $n \geq 1$, define the function $\phi_n(t) = (t - T/2)^{n-1} \exp(t - T/2)$. It is well-known that the set $\{\phi_n\}_{n=1}^\infty$ is complete in $L^2(0, T)$. Employing the Gram-Schmidt orthonormalization process on this set, we obtain an orthonormal basis of $L^2(0, T)$. We denote this basis by $\{\Psi_n\}_{n=1}^\infty$. We have the proposition

Proposition 2.1 (see [18]). *The basis $\{\Psi_n\}_{n=1}^\infty$ satisfies the following properties:*

1. Ψ_n is not identically zero for all $n \geq 1$,
2. For all $m, n \geq 1$

$$s_{mn} = \int_0^T \Psi'_n(t) \Psi_m(t) dt = \begin{cases} 1 & \text{if } m = n, \\ 0 & \text{if } n < m. \end{cases}$$

As a result, for all integer $N > 0$, the matrix $S = (s_{mn})_{m,n=1}^N$, is invertible.

Recall the Fourier coefficients of the function $v(\mathbf{x}, t)$

$$v_n(\mathbf{x}) = \int_0^T v(\mathbf{x}, t) \Psi_n(t) dt \quad \text{for all } \mathbf{x} \in \Omega. \quad (7)$$

We have

$$v(\mathbf{x}, t) = \sum_{n=1}^\infty v_n(\mathbf{x}) \Psi_n(t) \quad \text{for all } (\mathbf{x}, t) \in \Omega_T.$$

Fix a number $N > 0$. We approximate the function $v(\mathbf{x}, t)$ by the partial sum

$$v(\mathbf{x}, t) = \sum_{n=1}^N v_n(\mathbf{x}) \Psi_n(t) \quad \text{for all } (\mathbf{x}, t) \in \Omega_T. \quad (8)$$

In this approximation context,

$$v(\mathbf{x}, 0) = \sum_{n=1}^N v_n(\mathbf{x}) \Psi_n(0) \quad \text{for all } \mathbf{x} \in \Omega \quad (9)$$

and

$$v_t(\mathbf{x}, t) = \sum_{n=1}^N v_n(\mathbf{x}) \Psi'_n(t) \quad \text{for all } \mathbf{x} \in \Omega. \quad (10)$$

Plugging (8), (9) and (10) into (6), we have

$$\sum_{n=1}^N v_n(\mathbf{x}) \Psi'_n(t) = \sum_{n=1}^N L v_n(\mathbf{x}) \Psi_n(t) - \frac{L f(\mathbf{x})}{f(\mathbf{x})} \sum_{n=1}^N v_n(\mathbf{x}) \Psi_n(t) + \sum_{n,l=1}^N \frac{v_n(\mathbf{x}) \Psi_n(0)}{f(\mathbf{x})} v_l(\mathbf{x}) \Psi_l(t)$$

for all $(\mathbf{x}, t) \in \Omega_T$. For each $m \in \{1, 2, \dots, N\}$, multiply both sides of the equation above by $\Psi_m(t)$ and integrate the resulting equation with respect to t . Noting that

$$\int_0^T \Psi_n(t) \Psi_m(t) dt = \delta_{m-n},$$

we have for each $m \in \{1, \dots, N\}$,

$$L v_m(\mathbf{x}) - \sum_{n=1}^N s_{mn} v_n(\mathbf{x}) - \frac{L f(\mathbf{x})}{f(\mathbf{x})} v_m(\mathbf{x}) + \sum_{n=1}^N \frac{\Psi_n(0)}{f(\mathbf{x})} v_n(\mathbf{x}) v_m(\mathbf{x}) = 0 \quad (11)$$

for all $\mathbf{x} \in \Omega$. On the other hand, for each $m \in \{1, \dots, N\}$, the function $v_m(\mathbf{x})$ satisfies the following constraints

$$\begin{aligned} v_m(\mathbf{x}) &= F_m(\mathbf{x}) = \int_0^T F_t(\mathbf{x}, t) \Psi_m(t) dt, \\ \partial_\nu v_m(\mathbf{x}) &= G_m(\mathbf{x}) = \int_0^T G_t(\mathbf{x}, t) \Psi_m(t) dt \end{aligned} \quad (12)$$

for all $\mathbf{x} \in \partial\Omega$, $m \in \{1, \dots, N\}$.

Remark 2.2. From now on, we consider F_m and G_m as the indirect given data. Let F_m^* and G_m^* be the data without noise. The corresponding noisy data, with noise level $\delta > 0$, is given by

$$F_m^\delta(\mathbf{x}) = F_m^*(\mathbf{x})(1 + \delta \text{rand}(\mathbf{x})), \quad G_m^\delta(\mathbf{x}) = G_m^*(\mathbf{x})(1 + \delta \text{rand}(\mathbf{x})) \quad (13)$$

for each $m \in \{1, \dots, N\}$ where rand is the function of uniformly distributed random numbers in the range $[-1, 1]$. In this paper, we test our numerical method from simulated data with 10% noise.

In summary, we have proved the following proposition.

Proposition 2.2. Fix $N > 0$. Assume that the function $v(\mathbf{x}, t)$, $(\mathbf{x}, t) \in \Omega_T$, can be well-approximated by the expression in (8) with the function $v_n(\mathbf{x})$, $n \in \{1, 2, \dots, N\}$, given in (7). Then the Fourier coefficients v_n satisfies the over-determined system of partial differential equations (11)–(12).

3. The method to solve Problem 1.1

Solving Problem 1.1 is reduced to solve the system of nonlinear system of partial differential equation (11)–(12).

3.1. An iterative process

Solving the nonlinear system (11)–(12) is challenging. We propose the following iterative method, in which a predictor-corrector procedure is applied. The first predictor, named as $V^{(0)}$, is set to be the solution of the linear system obtained by removing from (11) the nonlinear term. More precisely, we set $V^{(0)} = (v_1^{(0)}, \dots, v_N^{(0)})^T$ as the solution of

$$L v_m^{(0)}(\mathbf{x}) - \sum_{n=1}^N s_{mn} v_n^{(0)}(\mathbf{x}) - \frac{L f(\mathbf{x})}{f(\mathbf{x})} v_m^{(0)}(\mathbf{x}) = 0 \quad \text{for all } \mathbf{x} \in \Omega \quad (14)$$

and

$$v_m^{(0)}(\mathbf{x}) = F_m(\mathbf{x}), \partial_\nu v_m^{(0)}(\mathbf{x}) = G_m(\mathbf{x}) \quad \text{for all } \mathbf{x} \in \partial\Omega \quad (15)$$

for $m \in \{1, \dots, N\}$. Next, by induction, assume that $V^{(p)}$ is known for some positive integer p , we find $V^{(p+1)}$ by solving the equation obtained from (11) by replacing v_m in the nonlinear term by its approximation $v_m^{(p)}$. That means, $V^{(p+1)} = (v_1^{(p+1)}, \dots, v_N^{(p+1)})^T$ is set to be the solution of

$$Lv_m^{(p+1)}(\mathbf{x}) - \sum_{n=1}^N s_{mn} v_n^{(p+1)}(\mathbf{x}) - \frac{Lf(\mathbf{x})}{f(\mathbf{x})} v_m^{(p+1)}(\mathbf{x}) + \sum_{n=1}^N \frac{\Psi_n(0)}{f(\mathbf{x})} v_n^{(p+1)}(\mathbf{x}) v_m^{(p)}(\mathbf{x}) = 0 \quad \text{for all } \mathbf{x} \in \Omega \quad (16)$$

and

$$v_m^{(p+1)}(\mathbf{x}) = F_m(\mathbf{x}), \quad \partial_\nu v_m^{(p+1)}(\mathbf{x}) = G_m(\mathbf{x}) \quad \text{for all } \mathbf{x} \in \partial\Omega \quad (17)$$

for each $m \in \{1, \dots, N\}$.

Due to the presence of the lateral Cauchy data, both problems (14)–(15) and (16)–(17) are over-determined. We employ the quasi-reversibility method to solve them.

3.2. The quasi-reversibility method

We next recall the quasi-reversibility method to solve systems of partial differential equations with Cauchy boundary data. The two systems of elliptic partial differential equations (14)–(15) and (16)–(17) are over-determined due to both Dirichlet and Neumann boundary conditions imposed. We use the quasi-reversibility method to solve them. A general form of these systems can be read as

$$\begin{cases} \operatorname{div}(A\nabla V) + BV &= 0 & \mathbf{x} \in \Omega, \\ V &= \mathcal{F} & \mathbf{x} \in \partial\Omega, \\ \partial_\nu V &= \mathcal{G} & \mathbf{x} \in \partial\Omega \end{cases} \quad (18)$$

where A is introduced in Section 1 and B is a $N \times N$ matrix valued function in $L^\infty(\Omega)$. We have the proposition whose proof closely follows that of Theorem 3.1 in [19].

Proposition 3.1. *Fix $\epsilon > 0$. Then, the functional*

$$J_\epsilon(V) = \int_\Omega |\operatorname{div}(A\nabla V) + BV|^2 d\mathbf{x} + \int_{\partial\Omega} |V - \mathcal{F}|^2 d\sigma(\mathbf{x}) + \int_{\partial\Omega} |\partial_\nu V - \mathcal{G}|^2 d\sigma(\mathbf{x}) + \epsilon \|V\|_{H^2(\Omega)}^2 \quad (19)$$

has a unique minimizer on $H^2(\Omega)$. This minimizer V_ϵ is called the regularized solution of (18).

In summary, we propose Algorithm 1 to solve Problem 1.1 via solving (11)–(12) by the quasi-reversibility method. The following inequality plays an important role for the convergence of the quasi-reversibility method.

Lemma 3.1 (Carleman estimate). *Let the number $b > R$. Then there exist numbers $p_0 \geq 1$ and $\lambda \geq 1$ depending only on $\mu, b, d, R, \|A\|_{L^\infty(\Omega)^{d \times d}}$ such that the following Carleman estimate holds:*

$$\int_\Omega |\operatorname{div}(A\nabla u)|^2 \exp[2\lambda(x_d + b)^p] d\mathbf{x} \geq C\lambda \int_\Omega [|\nabla u|^2 + \lambda^2 u^2] \exp[2\lambda(x_d + b)^p] d\mathbf{x}, \quad (20)$$

for all $\lambda \geq \lambda_0, p \geq p_0$ and $u \in H^2(\Omega)$ with $u = \partial_\nu u = 0$ on $\partial\Omega$. Here, the constant C depends only on $\mu, b, d, R, \|A\|_{L^\infty(\Omega)^{d \times d}}$.

Lemma 3.1 is a direct consequence of [19, Theorem 4.1]. We do not repeat the proof in this paper.

Theorem 3.1 (The convergence of the quasi-reversibility method for (18)). *Assume that there uniquely exists a true solution to (18) with the boundary data \mathcal{F} and \mathcal{G} replaced by the corresponding noiseless ones, denoted by \mathcal{F}^* and \mathcal{G}^* respectively. Let \mathcal{F}^δ and \mathcal{G}^δ be the corresponding noisy data for some $\delta > 0$. Assume that there exists an “error” vector valued function \mathcal{E} such that*

$$\mathcal{E} = \mathcal{F}^\delta - \mathcal{F}^* \quad \text{and} \quad \partial_\nu \mathcal{E} = \mathcal{G}^\delta - \mathcal{G}^* \quad (21)$$

on $\partial\Omega$ and assume that

$$\|\mathcal{E}\|_{H^2(\Omega)} \leq \delta \quad (22)$$

Then, V_ϵ^δ , the regularized solution to (18), satisfies the estimate

$$\|V_\epsilon^\delta - V^*\|_{H^1(\Omega)^N}^2 \leq C(\delta^2 + \epsilon\|V^*\|_{H^2(\Omega)^N}^2). \quad (23)$$

Remark 3.1. The convergence for the quasi-reversibility method guaranteed by Theorem 3.1 is similar to that in [19, Theorem 5.1]. The main difference of two results is in the objective functional is minimized subject to some boundary constraints while in the current paper, such constraints are relaxed by adding the two boundary integrals in (19).

Proof of Theorem 3.1. Since V_ϵ^δ is the regularized solution to (18), it is the minimizer of J_ϵ , defined in (19). Hence, for all $\phi \in H^2(\Omega)^N$, we have

$$\begin{aligned} \langle \operatorname{div}(A\nabla V_\epsilon^\delta) + BV_\epsilon^\delta, \operatorname{div}(A\nabla\phi) + B\phi \rangle_{L^2(\Omega)^N} \\ + \langle V_\epsilon^\delta - \mathcal{F}^\delta, \phi \rangle_{L^2(\partial\Omega)^N} + \langle \partial_\nu V_\epsilon^\delta - \mathcal{G}^\delta, \partial_\nu\phi \rangle_{L^2(\partial\Omega)^N} + \epsilon \langle V_\epsilon^\delta, \phi \rangle_{H^2(\Omega)^N} = 0 \end{aligned} \quad (24)$$

for all $\phi \in H^2(\Omega)^N$. On the other hand, since V^* is the true solution to (18)

$$\begin{aligned} \langle \operatorname{div}(A\nabla V^*) + BV^*, \operatorname{div}(A\nabla\phi) + B\phi \rangle_{L^2(\Omega)^N} \\ + \langle V^* - \mathcal{F}^*, \phi \rangle_{L^2(\partial\Omega)^N} + \langle \partial_\nu V^* - \mathcal{G}^*, \partial_\nu\phi \rangle_{L^2(\partial\Omega)^N} + \epsilon \langle V^*, \phi \rangle_{H^2(\Omega)^N} = \epsilon \langle V^*, \phi \rangle_{H^2(\Omega)^N} \end{aligned} \quad (25)$$

for all $\phi \in H^2(\Omega)^N$. Taking the difference of (24) and (25), we have

$$\begin{aligned} \langle \operatorname{div}(A\nabla W) + BW, \operatorname{div}(A\nabla\phi) + B\phi \rangle_{L^2(\Omega)^N} + \langle W - (\mathcal{F}^\delta - \mathcal{F}^*), \phi \rangle_{L^2(\partial\Omega)^N} \\ + \langle \partial_\nu W - (\mathcal{G}^\delta - \mathcal{G}^*), \partial_\nu\phi \rangle_{L^2(\partial\Omega)^N} + \epsilon \langle W, \phi \rangle_{H^1(\Omega)^N} = -\epsilon \langle V^*, \phi \rangle_{H^2(\Omega)^N} \end{aligned} \quad (26)$$

where $W = V_\epsilon^\delta - V^*$ for all $\phi \in H^2(\Omega)^N$. Using

$$\phi = W - \mathcal{E} = V_\epsilon^\delta - V^* - \mathcal{E} \quad (27)$$

as a test function in (26) and using (21), we have

$$\begin{aligned} \|\operatorname{div}(A\nabla\phi) + B\phi\|_{L^2(\Omega)^N}^2 + \langle \operatorname{div}(A\nabla\mathcal{E}) + B\mathcal{E}, \operatorname{div}(A\nabla\phi) + B\phi \rangle_{L^2(\Omega)^N} + \|\phi\|_{L^2(\partial\Omega)^N}^2 + \|\partial_\nu\phi\|_{L^2(\partial\Omega)^N}^2 \\ + \epsilon \|\phi\|_{H^2(\Omega)^N}^2 + \epsilon \langle \mathcal{E}, \phi \rangle_{H^2(\Omega)^N} = -\epsilon \langle V^*, \phi \rangle_{H^2(\Omega)^N}. \end{aligned}$$

Applying the inequality $|\langle u, v \rangle| \leq 1/2(\|u\|^2 + \|v\|^2)$, (22) and the trace theory, we have

$$\|\operatorname{div}(A\nabla\phi) + B\phi\|_{L^2(\Omega)^N}^2 \leq C(\delta^2 + \epsilon\|V^*\|_{H^2(\Omega)^N}^2). \quad (28)$$

Here, C is a generic constant that might change from estimate to estimate. Choose $b > R$, $\lambda > \lambda_0$, $p \geq p_0$ where b , λ_0 and p_0 are as in Lemma 3.1. It is not hard to verify that the function ϕ satisfies the homogenous boundary conditions $\phi = \partial_\nu\phi = 0$ on $\partial\Omega \times [0, T]$. Using the Carleman estimate in Lemma 3.1, we can bound the left hand side of (28) as follows

$$\begin{aligned} \int_\Omega |\operatorname{div}(A\nabla\phi) + B\phi|^2 dx &\geq \exp(-2\lambda(R+b)) \int_\Omega \exp(2\lambda(x_d+b)) |\operatorname{div}(A\nabla\phi) + B\phi|^2 dx \\ &\geq C \int_\Omega [\exp(2\lambda(x_d+b)) |\operatorname{div}(A\nabla\phi)|^2 - \exp(2\lambda(x_d+b)) |B\phi|^2] dx \\ &\geq C \int_\Omega [\exp(2\lambda(x_d+b)) (\lambda^3 |\phi|^2 + \lambda |\nabla\phi|^2) - \exp(2\lambda(x_d+b)) |B\phi|^2] dx. \end{aligned}$$

Choosing λ sufficiently large, since $B \in L^\infty(\Omega)$, we have

$$\|\operatorname{div}(A\nabla\phi) + B\phi\|_{L^2(\Omega)^N}^2 \geq C\|\phi\|_{H^1(\Omega)^N}^2.$$

This, together with (27) and (28), implies

$$\|V_\epsilon^\delta - V^*\|_{H^1(\Omega)^N}^2 \leq C(\delta^2 + \epsilon\|V^*\|_{H^2(\Omega)^N}^2).$$

The theorem is proved. \square

Theorem 3.1 guarantees that Steps 2 and 4 in Algorithm 1 provide good approximations of the sequence $\{c_p^\delta\}_{p=1}^\infty$ in comparison to the sequence $\{c_p^*\}_{p=1}^\infty$ with the Lipschitz rate provided that $\epsilon = O(\delta^2)$ as $\delta \rightarrow 0^+$. If the sequence $\{c_p^*\}_{p=1}^\infty$ converges to the solution of Problem 1.1, Algorithm 1 yields a numerical procedure to solve it. This convergence is verified numerically in Section 5.

3.3. The procedure to solve the coefficient inverse problem for parabolic equations

By Proposition 2.2, the strategy to solve (11)–(12) described in Section 3.1 and the convergence of the quasi-reversibility method, see Theorem 3.1, we propose Algorithm 1 to reconstruct the coefficient $c(\mathbf{x})$, $\mathbf{x} \in \Omega$.

Algorithm 1 The procedure to solve Problem 1.1

- 1: Choose a number N . Construct the functions Ψ_m , $1 \leq m \leq N$, and compute the matrix S as in Proposition 2.1. Fix $\epsilon > 0$.
- 2: Find the regularized solution $V^{(0)}$ of (14)–(15).
- 3: Compute $v^{(0)}$ via (8) and $c^{(0)}$ via (5).
- 4: Assume that we know $V^{(p)}$ and $c^{(p)}$. Set $V^{(p+1)}$ as the regularized solution to (16)–(17).
- 5: Compute $v^{(p+1)}$ via (8) and $c^{(p+1)}$ via (5).
- 6: Define

$$\mathcal{E}(p) = \frac{\|c^{(p)} - c^{(p+1)}\|_{L^\infty(\Omega)}}{\|c^{(p+1)}\|_{L^\infty(\Omega)}}.$$

Choose $c = c^{(p^*)}$ for p^* such that $\mathcal{E}(p^*)$ is sufficiently small.

Remark 3.2. Unlike the widely used numerical method to solve ill-posed inverse problems, we do not require a good initial guess for the true coefficient $c(\mathbf{x})$. Our first approximation is computed in Step 2 and Step 3 of Algorithm 1. It is shown in Section 5 that the functions $c^{(0)}$ are acceptable in Tests 1, 3 and 4. In contrast, our computed $c^{(0)}$ is poor in Test 2. However, the error is automatically corrected when we find $c^{(1)}$ in Step 4 and Step 5.

4. The implementation using the finite difference method

We test our method in the simple case when $d = 2$, $\Omega = (-1, 1)^2$, $L = \Delta$ is the Laplacian and $f(\mathbf{x}) = 1$.

4.1. The forward problem

To generate the simulated data, we solve the forward problem of Problem 1.1. That means we compute the solution $u(\mathbf{x}, t)$ to (1) on the whole plane \mathbb{R}^2 , given $c(\mathbf{x})$. Instead of doing so, we solve an analog of (1) on a domain $\Omega_1 = (R_1, R_1)^2$ where $R_1 = 3 > R = 1$. To guarantee the correctness of this domain approximation, we take T small, $T = 0.3$, so that the heat generated by $c(\mathbf{x})$ does not have enough time to hit the boundary of Ω_1 as $t \in [0, T]$. In other words, we solve the equation

$$\begin{cases} u_t(\mathbf{x}, t) = \Delta u(\mathbf{x}, t) + c(\mathbf{x})u(\mathbf{x}, t) & \mathbf{x} \in \Omega_1, t \in [0, T], \\ u(\mathbf{x}, t) = f(\mathbf{x}) & \mathbf{x} \in \partial\Omega_1, t \in [0, T], \\ u(\mathbf{x}, 0) = f(\mathbf{x}) & \mathbf{x} \in \Omega_1. \end{cases} \quad (29)$$

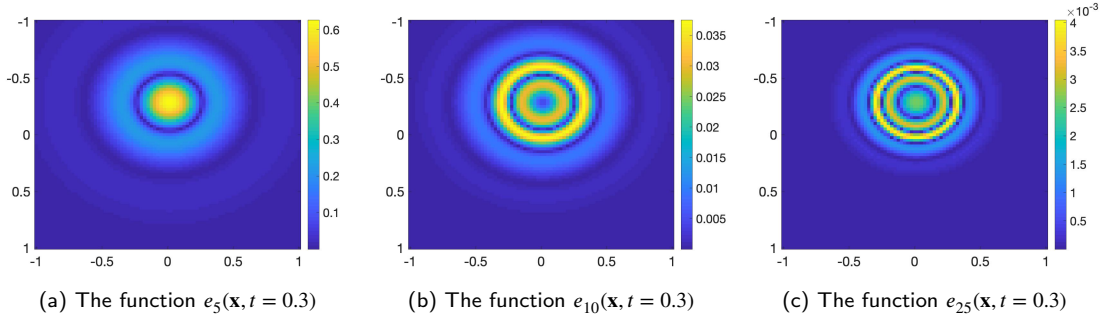


Figure 1: The difference of the function $v(\mathbf{x}, t)$ and the function $\sum_{n=1}^N v_n(\mathbf{x})\Psi_n(t)$ when $t = 0.3$.

Here, we choose the time-independent Dirichlet boundary data for the simplicity. In this paper, we solve problem (29) by the implicit method using finite difference. In the finite difference scheme, we find the function $u(\mathbf{x}, t)$ on the grid of points

$$\left\{ (x_i = -R_1 + (i-1)d_{x_1}, y_j = -R_1 + (j-1)d_{x_1}, (l-1)d_t) : 1 \leq i, j \leq N_1, 1 \leq l \leq N_t \right\} \subset \bar{\Omega}_1 \times [0, T]$$

where N_1 and N_t are two large integers, $d_{x_1} = 2R_1/(N_1 - 1)$ and $d_t = T/(N_t - 1)$. In our computational program, N_1 is set to be 240 and $N_t = 100$. Having the function $u(\mathbf{x}, t)$ for all $\mathbf{x} \in \Omega_1$ and $t \in [0, T]$ in hand, we can directly extract the data $F(\mathbf{x}, t) = u(\mathbf{x}, t)$ and $G(\mathbf{x}, t) = \partial_\nu u(\mathbf{x}, t)$ on $\partial\Omega \times [0, T]$.

4.2. The inverse problem

In this section, we present how to implement Algorithm 1 in the finite difference scheme. Similarly to the previous section, we define and then compute the function c on a uniform grid of points

$$\{(x_i = -R + (i-1)d_x, y_j = -R + (j-1)d_x, (l-1)d_t) : 1 \leq i, j \leq N_x, 1 \leq l \leq N_t\} \subset \bar{\Omega} \times [0, T]$$

where N_x and N_t are two large integers, $d_x = 2R/(N_x - 1)$ and $d_t = T/(N_t - 1)$. In all numerical tests in Section 5, we take $N_x = 80$ and $N_t = 100$.

We next present each step of Algorithm 1.

Step 1. In this step, to choose “truncation” number N . To do so, we take a “reference” function v in one of the examples in Section 5 and then compute the absolute difference

$$e_N(\mathbf{x}, t) = \left| v(\mathbf{x}, t) - \sum_{n=1}^N v_n(\mathbf{x})\Psi_n(t) \right| \quad \text{for all } \mathbf{x} \in \Omega, t \in [0, T].$$

We observe that the larger N , the smaller $\|e_N\|_{L^\infty(\Omega \times [0, T])}$. We examine the function e_N when $N = 5$, $N = 10$ and $N = 25$, see Figure 1. It is evident from (1c) that when $N = 25$, $\|e_N\|_{L^\infty}$ is sufficiently small, about $4(10^{-3})$.

As a result, we choose $N = 25$. We use this choice of N for all numerical tests. We observe that using higher N does not improve the quality of the reconstructed coefficient $c(\mathbf{x})$. Also in Step 1 of Algorithm 1, we choose the regularized number $\epsilon = 10^{-9}$.

Step 2. Compute the vector valued function $V^{(0)}$, which is set to be the minimizer of the functional, due to the quasi-reversibility method,

$$J_\epsilon^{(0)}(V) = \sum_{m=1}^N \left[\int_{\Omega} \left| \Delta v_m(\mathbf{x}) - \sum_{n=1}^N s_{mn} v_n(\mathbf{x}) - \frac{\Delta f(\mathbf{x})}{f(\mathbf{x})} v_m(\mathbf{x}) \right|^2 d\mathbf{x} + \int_{\partial\Omega} |v_m(\mathbf{x}) - F_m(\mathbf{x})|^2 d\sigma(\mathbf{x}) + \int_{\partial\Omega} |\partial_\nu v_m(\mathbf{x}) - G_m(\mathbf{x})|^2 d\sigma(\mathbf{x}) + \epsilon \int_{\Omega} (|v_m(\mathbf{x})|^2 + |\nabla v_m(\mathbf{x})|^2) d\mathbf{x} \right]. \quad (30)$$

Here, we replace the term $\|V\|_{H^2(\Omega)}^2$ in (19) by the term $\|V\|_{H^1(\Omega)}^2$. This is because the $H^1(\Omega)$ -norm is easier to work with computationally than the $H^2(\Omega)$ -norm. On the other hand, we have not observed any instabilities probably because the number 80×80 of grid points we use is not too large and all norms in finite dimensional spaces are equivalent. We now identify $\{v_m(x_i, y_j) : 1 \leq i, j, N_x, 1 \leq m \leq N\}$ by the $N_x^2 N$ dimensional vector \mathbf{v} whose the \mathbf{i}^{th} entry is given by

$$\mathbf{v}_{\mathbf{i}} = v_m(x_i, y_j). \quad (31)$$

Here, (i, j, m) is such that

$$\mathbf{i} = (i - 1)N_x N + (j - 1)N + m. \quad (32)$$

Then, by approximate all differential operators in the right hand side of (30) by the corresponding finite difference version, we have

$$J_\epsilon^{(0)}(V) = d_x^2 |\mathfrak{L}\mathbf{v}|^2 + d_x |\mathfrak{D}_1 \mathbf{v} - \mathfrak{F}|^2 + d_x |\mathfrak{D}_2 \mathbf{v} - \mathfrak{G}|^2 + \epsilon d_x^2 |\mathbf{v}|^2 + \epsilon d_x^2 |D_x \mathbf{v}|^2 + \epsilon d_x^2 |D_y \mathbf{v}|^2 \quad (33)$$

where the matrices \mathfrak{L} , \mathfrak{D}_1 , \mathfrak{D}_2 , D_x and D_y and the vectors \mathfrak{F} and \mathfrak{G} are described below. The $N_x^2 N \times N_x^2 N$ matrix \mathfrak{L} is given by

1. $\mathfrak{L}_{\mathbf{ij}} = -4/d_x^2 - s_{mm} - \Delta f(x_i, y_j)/f(x_i, y_j)$ if $\mathbf{i} = \mathbf{j} = (i - 1)N_x N + (j - 1)N + m$;
2. $\mathfrak{L}_{\mathbf{ij}} = 1/d_x^2$ if $\mathbf{i} = (i - 1)N_x N + (j - 1)N + m$ and $\mathbf{j} = (i \pm 1 - 1)N_x N + t(j \pm 1 - 1)N + m$;
3. $\mathfrak{L}_{\mathbf{ij}} = -s_{mn}$ if $\mathbf{i} = (i - 1)N_x N + (j - 1)N + m$ and $\mathbf{j} = (i - 1)N_x N + (j - 1)N + n, n \neq m$;
4. all other entries of \mathfrak{L} are 0;

for all $2 \leq i, j \leq N_x - 1, 1 \leq m \leq N$. The $N_x^2 N \times N_x^2 N$ matrix \mathfrak{D}_1 is given by

1. $(\mathfrak{D}_1)_{\mathbf{ij}} = 1$ if $\mathbf{i} = \mathbf{j} = (i - 1)N_x N + (j - 1)N + m$ for $i \in \{1, N_x\}, 1 \leq j \leq N_x, 1 \leq m \leq N$;
2. $(\mathfrak{D}_1)_{\mathbf{ij}} = 1$ if $\mathbf{i} = \mathbf{j} = (i - 1)N_x N + (j - 1)N + m$ for $1 \leq i \leq N_x, j \in \{1, N_x\}, 1 \leq m \leq N$;
3. all other entries of \mathfrak{D}_1 are 0.

The $N_x^2 N \times N_x^2 N$ matrix \mathfrak{D}_2 is given by

1. $(\mathfrak{D}_2)_{\mathbf{ij}} = 1/d_x$ if $\mathbf{i} = \mathbf{j} = (i - 1)N_x N + (j - 1)N + m$ for $i \in \{1, N_x\}, 1 \leq j \leq N_x, 1 \leq m \leq N$;
2. $(\mathfrak{D}_2)_{\mathbf{ij}} = -1/d_x$ if $\mathbf{i} = (i - 1)N_x N + (j - 1)N + m$ and $\mathbf{j} = (i + 1 - 1)N_x N + (j - 1)N + m$ for $i = 1, 1 \leq j \leq N_x, 1 \leq m \leq N$;
3. $(\mathfrak{D}_2)_{\mathbf{ij}} = -1/d_x$ if $\mathbf{i} = (i - 1)N_x N + (j - 1)N + m$ and $\mathbf{j} = (i - 1 - 1)N_x N + (j - 1)N + m$ for $i = N_x, 1 \leq j \leq N_x, 1 \leq m \leq N$;
4. $(\mathfrak{D}_2)_{\mathbf{ij}} = 1/d_x$ if $\mathbf{i} = \mathbf{j} = (i - 1)N_x N + (j - 1)N + m$ for $i \in \{1, N_x\}, j \in \{1, N_x\}, 1 \leq m \leq N$;
5. $(\mathfrak{D}_2)_{\mathbf{ij}} = -1/d_x$ if $\mathbf{i} = (i - 1)N_x N + (j - 1)N + m$ and $\mathbf{j} = (i - 1)N_x N + (j + 1 - 1)N + m$ for $1 \leq i \leq N_x, j = 1, 1 \leq m \leq N$;
6. $(\mathfrak{D}_2)_{\mathbf{ij}} = -1/d_x$ if $\mathbf{i} = (i - 1)N_x N + (j - 1)N + m$ and $\mathbf{j} = (i - 1)N_x N + (j - 1 - 1)N + m$ for $1 \leq i \leq N_x, j = N_x, 1 \leq m \leq N$;
7. all other entries of \mathfrak{D}_2 are 0.

The $N_x^2 N \times N_x^2 N$ matrix D_x is given by

1. $(D_x)_{\mathbf{ij}} = 1/d_x$ if $\mathbf{i} = \mathbf{j} = (i - 1)N_x N + (j - 1)N + m$ for $1 \leq j \leq N_x - 1, 1 \leq j \leq N_x - 1, 1 \leq m \leq N$;

2. $(D_x)_{ij} = -1/d_x$ if $\mathbf{i} = (i-1)N_x N + (j-1)N + m$ and $\mathbf{j} = (i+1-1)N_x N + (j-1)N + m$ for $i = 1, 1 \leq j \leq N_x, 1 \leq m \leq N$;
3. all other entries of D_x are 0.

The $N_x^2 N \times N_x^2 N$ matrix D_y is given by

1. $(D_y)_{ij} = 1/d_x$ if $\mathbf{i} = \mathbf{j} = (i-1)N_x N + (j-1)N + m$ for $1 \leq j \leq N_x - 1, 1 \leq j \leq N_x - 1, 1 \leq m \leq N$;
2. $(D_y)_{ij} = -1/d_x$ if $\mathbf{i} = (i-1)N_x N + (j+1-1)N + m$ and $\mathbf{j} = (i+1-1)N_x N + (j-1)N + m$ for $i = 1, 1 \leq j \leq N_x, 1 \leq m \leq N$;
3. all other entries of D_y are 0.

The vector \mathfrak{F} is defined as

1. $\mathfrak{F}_i = F_m(x_i, y_j)$ if $\mathbf{i} = (i-1)N_x N + (j-1)N + m$ for $i \in \{1, N_x\}, 1 \leq j \leq N_x, 1 \leq m \leq N$;
2. all other entries of \mathfrak{F} are 0.

The vector \mathfrak{G} is defined as

1. $\mathfrak{G}_i = G_m(x_i, y_j)$ if $\mathbf{i} = (i-1)N_x N + (j-1)N + m$ for $i \in \{1, N_x\}, 1 \leq j \leq N_x, 1 \leq m \leq N$;
2. all other entries of \mathfrak{G} are 0.

Since ϵ is small (in our computational program $\epsilon = 10^{-9}$), to find the minimizer $V^{(0)}$ of the finite difference version of J_ϵ in (33), we solve the linear system

$$\left(\begin{bmatrix} \mathfrak{L} \\ \mathfrak{D}_1 \\ \mathfrak{D}_2 \end{bmatrix}^T \begin{bmatrix} \mathfrak{L} \\ \mathfrak{D}_1 \\ \mathfrak{D}_2 \end{bmatrix} + \epsilon(\text{Id} + D_x^T D_x + D_y^T D_y) \right) \mathbf{v} = \begin{bmatrix} \mathfrak{L} \\ \mathfrak{D}_1 \\ \mathfrak{D}_2 \end{bmatrix}^T \begin{bmatrix} \mathbf{0} \\ \mathfrak{F} \\ \mathfrak{G} \end{bmatrix}.$$

Having \mathbf{v} in hand, we can compute $V^{(0)} = (v_1^0, \dots, v_N^0)^T$ using (31) and (32).

Step 4. The implementation for this step is similar to that for Step 2. In this step, we minimize

$$J_\epsilon^{(p+1)}(V) = \sum_{m=1}^N \int_{\Omega} \left| \Delta v_m(\mathbf{x}) - \sum_{n=1}^N s_{mn} v_n(\mathbf{x}) - \frac{\Delta f(\mathbf{x})}{f(\mathbf{x})} v_m(\mathbf{x}) + \sum_{n=1}^N \frac{\Psi_n(0)}{f(\mathbf{x})} v_n(\mathbf{x}) v_m^{(p)}(\mathbf{x}) \right| + \int_{\partial\Omega} |\partial_\nu v_m(\mathbf{x}) - G_m(\mathbf{x})|^2 d\sigma(\mathbf{x}) + \epsilon \int_{\Omega} (|v_m(\mathbf{x})|^2 + |\nabla v_m(\mathbf{x})|^2) d\mathbf{x}. \quad (34)$$

To this end, we identify the vector valued function V by the vector \mathbf{v} as in (31) and (32) and then solve the linear system

$$\left(\begin{bmatrix} \mathcal{L} \\ \mathfrak{D}_1 \\ \mathfrak{D}_2 \end{bmatrix}^T \begin{bmatrix} \mathcal{L} \\ \mathfrak{D}_1 \\ \mathfrak{D}_2 \end{bmatrix} + \epsilon(\text{Id} + D_x^T D_x + D_y^T D_y) \right) \mathbf{v} = \begin{bmatrix} \mathcal{L} \\ \mathfrak{D}_1 \\ \mathfrak{D}_2 \end{bmatrix}^T \begin{bmatrix} \mathbf{0} \\ \mathfrak{F} \\ \mathfrak{G} \end{bmatrix}.$$

Here, the matrices $\mathfrak{D}_1, \mathfrak{D}_2, D_x$ and D_y and the vectors \mathfrak{F} and \mathfrak{G} are defined in the implementation section for Step 2. The $N_x^2 N \times N_x^2 N$ matrix \mathcal{L} is given by

1. $\mathcal{L}_{ij} = -4/d_x^2 - s_{mm} - \Delta f(x_i, y_j)/f(x_i, y_j) + v_m^{(p)}(x_i, y_j)\Psi_m(0)/f(x_i, y_j)$ if $\mathbf{i} = \mathbf{j} = (i-1)N_x N + (j-1)N + m$;
2. $\mathcal{L}_{ij} = 1/d_x^2$ if $\mathbf{i} = (i-1)N_x N + (j-1)N + m$ and $\mathbf{j} = (i \pm 1 - 1)N_x N + (j \pm 1 - 1)N + m$;
3. $\mathcal{L}_{ij} = -s_{mn} + v_n^{(p)}(x_i, y_j)\Psi_n(0)/f(x_i, y_j)$ if $\mathbf{i} = (i-1)N_x N + (j-1)N + m$ and $\mathbf{j} = (i-1)N_x N + (j-1)N + n, n \neq m$;

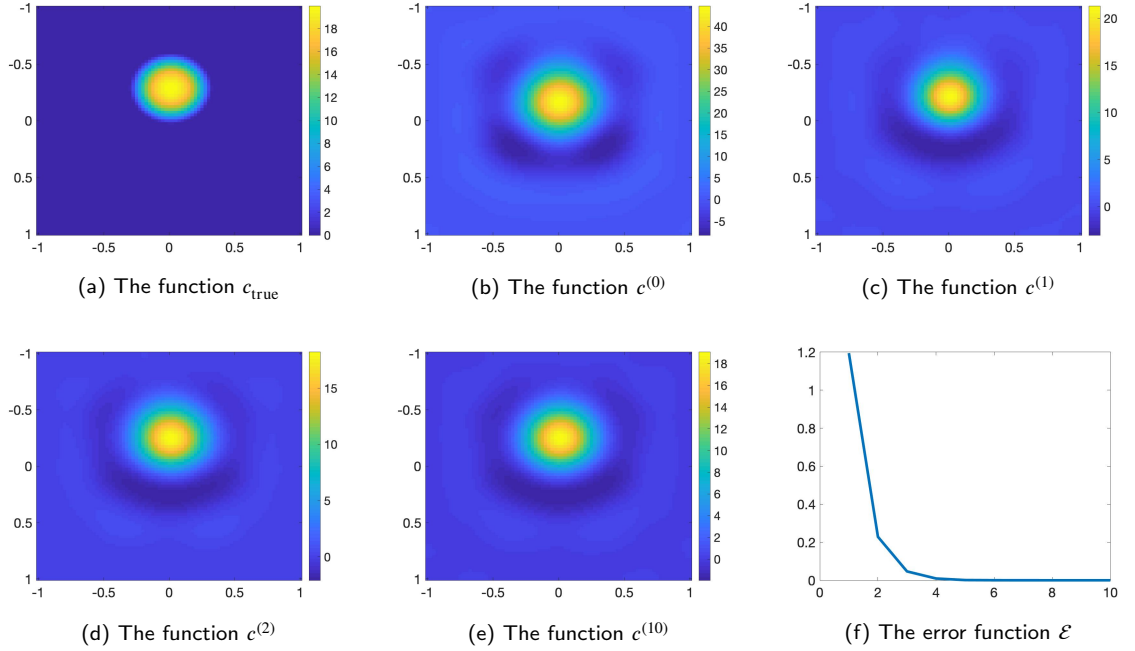


Figure 2: Test 1. The true coefficient and computed coefficient c . We observe from Figure 2b that $c^{(0)}$, computed by Step 2 of Algorithm 1, has good “image” of the true inclusion. It is evident from the graph of the error function \mathcal{E} , see Figure 2f, that the sequence $\{c^{(p)}\}_p$ converges fast.

4. all other entries of \mathcal{L} are 0;

for all $2 \leq i, j \leq N_x - 1$, $1 \leq m \leq N$. Having \mathbf{v} in hand, we can compute $V^{(p+1)} = (v_1^{(p+1)}, \dots, v_N^{(p+1)})^T$ using (31) and (32).

Steps 3, 5 and 6. The implementation of these steps is straight forward.

In the next section, we show some numerical results.

5. Numerical examples

The numerical results presented below are computed from the knowledge of $F_m(\mathbf{x}, t)$ and $G_m(\mathbf{x}, t)$, $m \in \{1, \dots, N\}$, on $\partial\Omega \times [0, 0.3]$ including 10% of noise where F_m and G_m are the boundary data in Remark 2.2. The number of truncation N is 25. The regularization parameter is $\epsilon = 10^{-9}$. The computational program is implemented by the finite difference method.

1. *Test 1.* The true function c_{true} has a smooth inclusion

$$c_{\text{true}} = \begin{cases} 0 & x^2 + (y + 0.3)^2 \geq 0.35^2 \\ 20e^{\frac{x^2 + (y + 0.3)^2}{x^2 + (y + 0.3)^2 - 0.23^2}} & x^2 + (y + 0.3)^2 \leq 0.35^2. \end{cases}$$

The numerical results for this case is displayed in Figure 2. One can observe in Figures 2b–2e that the circular shape and location of the inclusion can be successfully detected. The true maximal value of the function c_{true} is 20. The reconstructed maximal value of the function $c_{\text{comp}} = c^{(10)}$ is 19.07. The relative error is 4.65%.

2. *Test 2.* We test the case when the function c_{true} is a step function with two rectangular inclusions. This example is interesting since c_{true} is not smooth and the gap at the boundaries of the inclusions is high. The function c_{true}

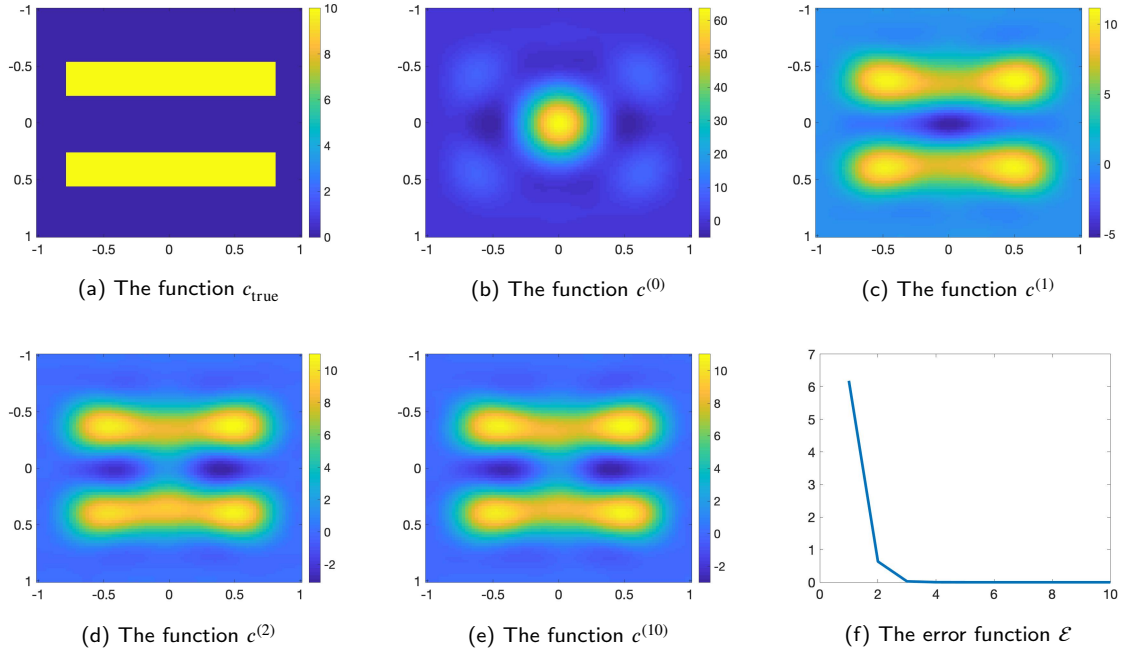


Figure 3: Test 2. The true coefficient and computed coefficient c . In this test, although the reconstructed coefficient $c^{(0)}$, see Figure 3b, is poor, the coefficient $c^{(1)}$ meets the expectation. It is evident from the graph of the error function \mathcal{E} , see Figure 3f, that the sequence $\{c^{(p)}\}_p$ converges fast.

is given by

$$c_{\text{true}} = \begin{cases} 10 & |x| < 0.8 \text{ and } |y \pm 0.4| < 0.15, \\ 0 & \text{otherwise.} \end{cases}$$

The numerical results for this case is displayed in Figure 3. One can observe in Figures 3c–3e that the reconstructed rectangular shape and location of the inclusion are satisfactory. The true maximal value of the function c_{true} is 10. The reconstructed maximal value of the function c_{comp} is 10.98. The relative error is 9.80%. Similarly to the previous test, it is evident from Figure 3f that our method converges fast.

3. *Test 3.* We test the case of two circular inclusions. In this case, the function c_{comp} is a step function with high gap at the boundary of the inclusions. The function c_{true} is given by

$$c_{\text{true}} = \begin{cases} 5 & x^2 + (y + 0.5)^2 < 0.23^2, \\ 8 & x^2 + (y - 0.5)^2 < 0.23^2, \\ 0 & \text{otherwise.} \end{cases}$$

The numerical results for this case is displayed in Figure 4. One can observe in Figure 4b that the circular shape and can be successfully detected at the first step. The true maximal value of the function c_{true} at the lower inclusion is 8 and the reconstructed one is 8.90. The relative error is 11.25%. The true maximal value of the function c_{true} at the upper inclusion is 5 and the reconstructed one is 5.24. The relative error is 4.80%. Figure 4f shows the stability of our method.

4. *Test 4.* We test the case when the function c_{true} is allowed to be negative. In this case, the function c_{comp} is the

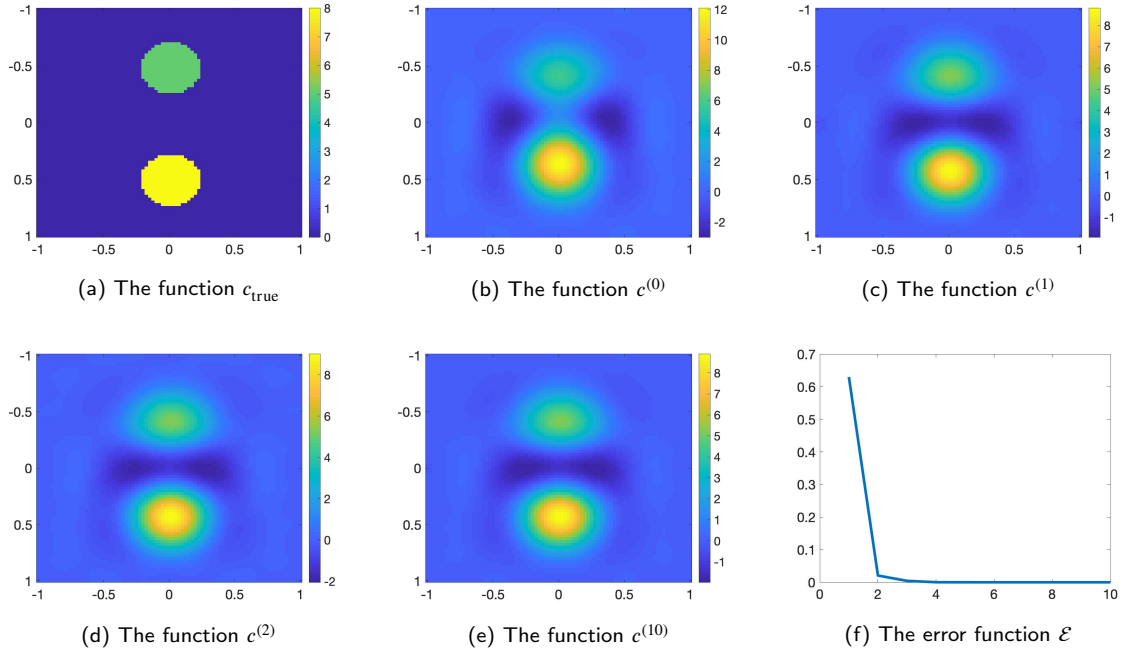


Figure 4: Test 3. The true coefficient and computed coefficient c . We already see both inclusions in the graph of the first approximation $c^{(0)}$, computed by Step 2 of Algorithm 1, see Figure 4b. It is evident from the graph of the error function \mathcal{E} , see Figure 4f, that the sequence $\{c^{(p)}\}_p$ converges fast.

letter X with a half is positive and another half is negative. The function c_{true} is given by

$$c_{\text{true}} = \begin{cases} 8 & |x| < 0.8, -0.8 < y \leq 0, |x \pm y| < 0.25, \\ -8 & |x| < 0.8, 0 < y < 0.8, |x \pm y| < 0.25, \\ 0 & \text{otherwise.} \end{cases}$$

The numerical results for this case is displayed in Figure 5. The reconstructed image of the letter X is acceptable. The true maximal positive value of the function c_{true} is 8 and the reconstructed one is 8.90. The relative error is 11.25%. The true minimal negative value of the function c_{true} is -8 and the reconstructed one is -7.93. The relative error is 0.88%. Again, Figure 5f shows the stability of our method.

Remark 5.1. It is evident from Figures 2c–5c that Algorithm 1 is robust in the sense that it provides good reconstructed coefficient c_{comp} after a few iterations. It is remarkable mentioning that, in all tests above, our method provides good numerical results without any advanced knowledge of the true coefficient c_{true} .

6. Concluding remarks

In this paper, we introduced a new approach to numerically compute the perfusion coefficient of a general parabolic equation. The method consists of deriving and solving a nonlinear system of coupled partial differential equations.

Acknowledgments

The author is grateful to Michael V. Klibanov for many fruitful discussions.

References

- [1] K. Cao, D. Lesnic, Simultaneous reconstruction of the perfusion coefficient and initial temperature from time-average integral temperature measurements, *Applied Mathematical Modelling* 68 (2019) 523–539.

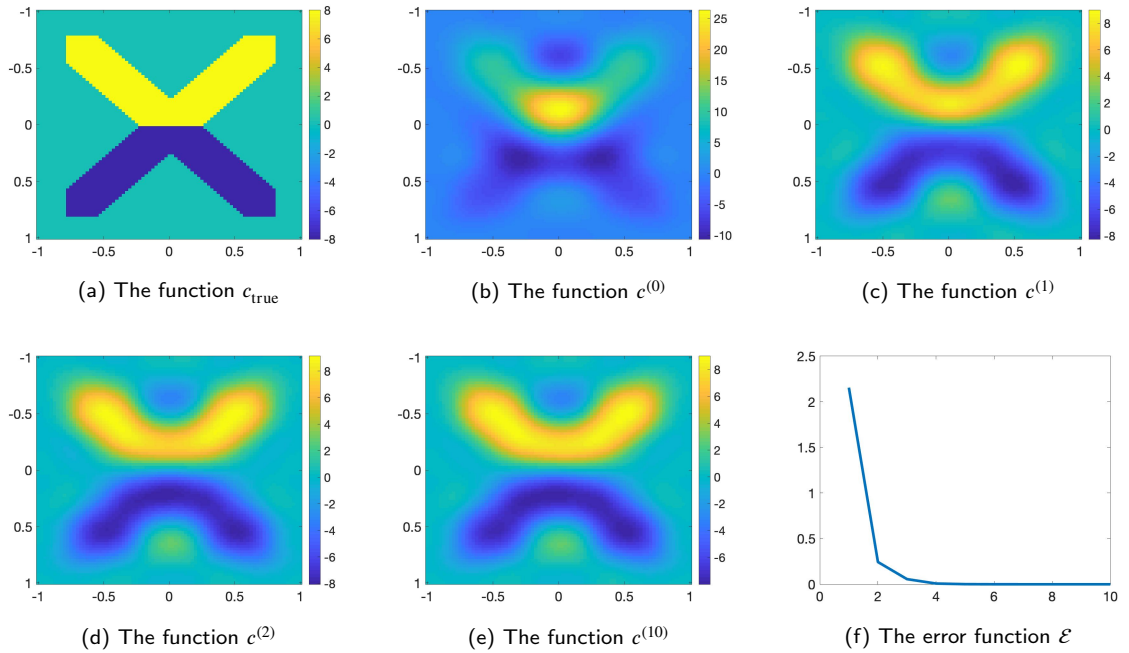


Figure 5: Test 4. The true coefficient and computed coefficient c . We already see the letter “X” in the graph of the first approximation $c^{(0)}$, computed by Step 2 of Algorithm 1, see Figure 5b. It is evident from the graph of the error function \mathcal{E} , see Figure 5f, that the sequence $\{c^{(p)}\}_p$ converges fast.

- [2] L. Beilina, M. V. Klibanov, Approximate Global Convergence and Adaptivity for Coefficient Inverse Problems, Springer, New York, 2012.
- [3] A. L. Bukhgeim, M. V. Klibanov, Uniqueness in the large of a class of multidimensional inverse problems, Soviet Math. Doklady 17 (1981) 244–247.
- [4] A. I. Prilepko, A. B. Kostin, On certain inverse problems for parabolic equations with final and integral observation, Russ. Acad. Sci. Sb. Math. 75 (1993) 473–490.
- [5] V. Isakov, Some inverse problems for the diffusion equation, Inverse Problems 15 (1) (1999) 3–10. doi:10.1088/0266-5611/15/1/004. URL <https://doi.org/10.1088/0266-5611/15/1/004>
- [6] M. V. Klibanov, A. G. Yagola, Convergent numerical methods for parabolic equations with reversed time via a new Carleman estimate, preprint (2019).
- [7] Q. Li, L. H. Nguyen, Recovering the initial condition of parabolic equations from lateral Cauchy data via the quasi-reversibility method,, preprint, arXiv:1902.07637 (2019).
- [8] H. T. Nguyen, V. A. Khoa, V. A. Vo, Analysis of a quasi-reversibility method for a terminal value quasi-linear parabolic problem with measurements, SIAM Journal on Mathematical Analysis 51 (2019) 60–85.
- [9] A. I. Prilepko, D. G. Orlovsky, I. A. Vasin, Methods for solving inverse problems in mathematical physics, Vol. 321, Pure and Applied Mathematics, Marcel Dekker, New York, 2000.
- [10] N. H. Tuan, V. V. Au, V. A. Khoa, D. Lesnic, Identification of the population density of a species model with nonlocal diffusion and nonlinear reaction, Inverse Problems 33 (2017) 055019.
- [11] L. Borcea, V. Druskin, A. V. Mamonov, M. Zaslavsky, A model reduction approach to numerical inversion for a parabolic partial differential equation, Inverse Problems 30 (2014) 125011.
- [12] K. Cao, D. Lesnic, Determination of space-dependent coefficients from temperature measurements using the conjugate gradient method, Numer Methods Partial Differential Eq. 34 (2018) 1370–1400.
- [13] Y. L. Keung, J. Zou, Numerical identifications of parameters in parabolic systems, Inverse Problems 14 (1998) 83–100.
- [14] L. Yang, J.-N. Yu, Y.-C. Deng, An inverse problem of identifying the coefficient of parabolic equation, Applied Mathematical Modelling 32 (2008) 1984–1995.
- [15] A. B. Bakushinskii, M. V. Klibanov, N. A. Koshev, Carleman weight functions for a globally convergent numerical method for ill-posed Cauchy problems for some quasilinear pdes, Nonlinear Anal. Real World Appl. 34 (2017) 201–224.
- [16] M. V. Klibanov, Carleman weight functions for solving ill-posed Cauchy problems for quasilinear PDEs, Inverse Problems 31 (2015) 125007.
- [17] P. M. Nguyen, L. H. Nguyen, A numerical method for an inverse source problem for parabolic equations and its application to a coefficient inverse problem, preprint, arXiv:1903.10628 (2019).
- [18] M. V. Klibanov, Convexification of restricted Dirichlet to Neumann map, J. Inverse and Ill-Posed Problems 25 (5) (2017) 669–685.
- [19] L. H. Nguyen, Q. Li, M. V. Klibanov, A convergent numerical method for a multi-frequency inverse source problem in inhomogenous media,

- to appear on *Inverse Problems and Imaging*, preprint, arXiv:1901.10047 (2019).
- [20] R. Lattès, J. L. Lions, *The Method of Quasireversibility: Applications to Partial Differential Equations*, Elsevier, New York, 1969.
 - [21] E. Bécache, L. Bourgeois, L. Franceschini, J. Dardé, Application of mixed formulations of quasi-reversibility to solve ill-posed problems for heat and wave equations: The 1d case, *Inverse Problems & Imaging* 9 (4) (2015) 971–1002.
 - [22] L. Bourgeois, Convergence rates for the quasi-reversibility method to solve the Cauchy problem for Laplace’s equation, *Inverse Problems* 22 (2006) 413–430.
 - [23] L. Bourgeois, J. Dardé, A duality-based method of quasi-reversibility to solve the Cauchy problem in the presence of noisy data, *Inverse Problems* 26 (2010) 095016.
 - [24] L. Bourgeois, D. Ponomarev, J. Dardé, An inverse obstacle problem for the wave equation in a finite time domain, *Inverse Probl. Imaging* 13 (2) (2019) 377–400.
 - [25] C. Clason, M. V. Klibanov, The quasi-reversibility method for thermoacoustic tomography in a heterogeneous medium, *SIAM J. Sci. Comput.* 30 (2007) 1–23.
 - [26] J. Dardé, Iterated quasi-reversibility method applied to elliptic and parabolic data completion problems, *Inverse Problems and Imaging* 10 (2016) 379–407.
 - [27] B. Kaltenbacher, W. Rundell, Regularization of a backwards parabolic equation by fractional operators, *Inverse Probl. Imaging* 13 (2) (2019) 401–430.
 - [28] M. V. Klibanov, F. Santosa, A computational quasi-reversibility method for Cauchy problems for Laplace’s equation, *SIAM J. Appl. Math.* 51 (1991) 1653–1675.
 - [29] M. V. Klibanov, Carleman estimates for global uniqueness, stability and numerical methods for coefficient inverse problems, *J. Inverse and Ill-Posed Problems* 21 (2013) 477–560.
 - [30] L. H. Nguyen, An inverse space-dependent source problem for hyperbolic equations and the Lipschitz-like convergence of the quasi-reversibility method, *Inverse Problems* 35 (2019) 035007.
 - [31] M. V. Klibanov, Carleman estimates for the regularization of ill-posed Cauchy problems, *Applied Numerical Mathematics* 94 (2015) 46–74.